J. Membrane Biol. 202, 161–170 (2004)
DOI: 10.1007/s00232-004-0727-2

The Journal of
Membrane
Biology

Opposite Cx32 and Cx26 Voltage-Gating Response to CO_2 Reflects Opposite Voltage-Gating Polarity

K.C. Young*, C. Peracchia
Department of Pharmacology and Physiology, School of Medicine and Dentistry, University of Rochester, 575 Elmwood Ave, Box 711 Rochester, NY 14620, USA

Received: 26 August 2004/Revised: 1 December 2004

Abstract. Previous studies have shown that the V_j-dependent gating behavior of gap junction channels is altered by CO_2 exposure. V_j-dependent channel closure is increased by CO_2 in some connexin channels and decreased in others. Since the former type of channels gate on the relatively negative side by V_j (negative gaters) and the latter at the positive side (positive gaters), it has been hypothesized that gating polarity determines the way CO_2 affects V_j closure. To test this hypothesis, we have studied the CO_2-mediated changes in V_j gating in channels made of Cx32, Cx26, or a Cx32 mutant (Cx32-N2D) in which asparagine (N) at position 2 was replaced with aspartate (D). With exposure to CO_2, Cx32 channels (negative gaters) show increased V_j-dependent closure, whereas Cx26 channels (positive gaters) respond in the opposite way to V_j. Additionally, Cx32-N2D channels (positive gaters) show decreased V_j closure with exposure to CO_2. The reciprocal Cx26 mutant, Cx26-D2N (negative gater), could not be tested because it did not express functional homotypic channels. The data support the hypothesis that polarity of fast V_j gating determines whether CO_2 increases or decreases the V_j dependent closure of gap junction channels.

Key words: Gap junction channels — pH gating — Chemical gating — Connexins — *Xenopus* oocytes

Introduction

Gap junction channels directly connect the cytoplasm of two adjacent cells, allowing for passage of ions and small molecules between the cells (Gilula, Reeves & Steinbach, 1972). Each channel is a dodecameric arrangement of the protein connexin, six from each cell. Connexin's NH_2-terminus (NT), cytoplasmic loop and COOH-terminus (CT) domains are on the cytoplasmic side of the junction. Each connexin has four transmembrane domains and two extracellular loops that are involved in cell-to-cell coupling (reviewed in Harris, 2001).

Gap junction channels are gated by transjunctional voltage (V_j; Spray, Harris & Bennett, 1981) and increases in $[Ca^{2+}]_i$ (Loewenstein, 1966; Rose & Loewenstein, 1975) or $[H^+]_i$ (Turin & Warner, 1977). The latter, termed chemical gating, may occur through domain interactions for Cx43 and possibly Cx40 (reviewed in Delmar et al., 2000) or via an intermediate protein for Cx32, possibly calmodulin (reviewed in Peracchia, 2004).

Several studies have identified the NT region, and part of the first extracellular loop as components of the voltage sensor for fast V_j gating (Rubin et al., 1992; Verselis, Ginter & Bargiello, 1994; Oh et al., 1999; Purnick et al., 2000). The polarity of fast V_j gating varies among connexins, as some connexin channels close at the relatively positive side of V_j (positive gaters) and others at the negative side (negative gaters; reviewed in Harris, 2001). It is well established that Cx32 and Cx26 undergo fast V_j gating with opposite polarity: Cx32 channels are negative gaters and Cx26 channels are positive gaters (Verselis et al., 1994; Oh et al., 1999; Purnick et al., 2000). Gap junction channels also have a slow V_j gate that is likely to be the same as the chemical gate (Bukauskas & Peracchia, 1997; Bukauskas, Vogel & Weingart, 1997; Peracchia, Wang & Peracchia, 1999). The slow V_j gate closes with negative potentials in all connexin channels tested and closes slowly but completely at the single-channel level (Bukauskas & Verselis, 2004). In contrast, the fast V_j gate closes the

**Present address:* Department of Neurology, University of Chicago, 5841 S. Maryland Ave, MC2030, Chicago, IL, 60637, USA
Correspondence to: K.C. Young; email: kyoung@neurology.bsd.uchicago.edu

channel rapidly but only partially, leaving a residual conductance of ~20% (Bukauskas & Peracchia, 1997).

Previous work has provided detailed analysis of fast V_j gating and chemical gating as separate mechanisms. Little interest has been shown in potential effects of chemical uncouplers, such as CO_2, on V_j gating. Werner et al. (1991) reported that Cx32 channels or Cx32 CT-truncated channels develop a V_j-dependence to 50 mV steps when exposed to 70% or 30% CO_2. Preliminary data have confirmed these results on Cx32 channels (Young & Peracchia, 2002). In addition, Peracchia et al. (2003b) have demonstrated that Cx45 channels also increase V_j closure (decrease of the ratio between steady-state and peak junctional conductance, G_{jss}/G_{jpeak}, for a given pulse) and speed of inactivation during CO_2-induced chemical uncoupling. In contrast, Cx40 and CT-truncated Cx40 channels (Peracchia et al., 2004), as well as Cx50 (Peracchia, *unpublished observations*), Cx37 (Peracchia, unpublished observations) and Cx26 (this study and Peracchia et al., 2003a) channels have recently been shown to decrease V_j-dependent channel closure with CO_2 application.

Based on the observation that CO_2 decreases V_j-dependent closure of positive-gating channels, such as Cx26, Cx37, Cx40, and Cx50, and increases that of negative gaters, such as Cx32 and Cx45, we have proposed the hypothesis that gating polarity determines the type of V_j-dependent gating response to CO_2 (Peracchia et al., 2004). To test this hypothesis, we have studied the V_j gating response to CO_2 of Cx32 and Cx26 channels, as well as that of channels made of a Cx32 mutant (Cx32-N2D) in which the asparagine (N) residue in position two was replaced by aspartate (D). This mutation has been previously shown to switch the gating polarity of Cx32 from negative to positive (Verselis, et al., 1994; Oh et al., 1999; Purnick et al., 2000). The present study uses changes in G_{jss}/G_{jmax} at a given V_j and changes in the Boltzmann fit parameters V_o (voltage at which half the conductance is inactivated) and G_{jmin} to assess CO_2-mediated effects on V_j gating. These data demonstrate that V_j closure of Cx32 and Cx26 channels responds in opposite ways to CO_2 application, and that a Cx32 mutation that switches fast V_j polarity (Cx32-N2D) also switches the V_j response to CO_2. A preliminary account of the three-minute CO_2 control data for Cx32 has appeared in abstract form (Young & Peracchia, 2002).

Materials and Methods

Site-directed Mutagenesis

For the mutants Cx32-N2D and Cx26-D2N, the second residue, N in Cx32 and D in Cx26, was replaced with D and N, respectively. The mutants were generated from the appropriate wild-type connexin in pBluescriptKS+ using standard molecular biology techniques (Sambrook et al., 1989). The following primers were used. Cx32-N2D Sense: 5′-gacgtcactagtatggactggacaggtcta and Cx26-D2N Sense: 5′-gacgtcactagtatgaattggggcacacta. The underlined residues form a *Spe1* site before the start codon. In combination with a T3 primer, one-step polymerase chain reaction generated fragments for subcloning. Successful point mutations were confirmed by direct sequence analysis.

For cRNA preparation Cx32 and Cx32-N2D were linearized with *Hind*III, while Cx26 and Cx26D2N were linearized with *Eco*RI. After a two hour in vitro transcription (T7 kit, mMessagemMachine, Ambion, Austin, TX), the cRNA was precipitated with LiCl for at least one hour and resuspended in 10 mM Tris-Cl pH 8.5 (Buffer EB, Qiagen, Valencia, CA). Concentration was determined by absorption at 260 nm.

Oocyte Preparation and Injection

Oocytes were prepared as previously described (Peracchia, Wang & Peracchia, 2000b).Briefly, oocytes were removed through a small incision in the abdomen of an adult female *Xenopus laevis* anesthetized by immersion in a 0.25% solution of sodium bicarbonate buffered tricaine (MS-222, Sigma, St. Louis, MO). Gentle agitation in nominally Ca^{2+}-free oocyte ringer OR2 supplemented with 2 mg/mL collagenase (Sigma) removed the follicular layer. The composition of OR2 is (in mM): NaCl 82.5, KCl 2, $MgCl_2$ 1, HEPES 5 at pH 7.6 with NaOH. The oocytes were returned to ND96 medium (in mM): NaCl 96, KCl 2, $CaCl_2$ 1.8, $MgCl_2$ 1, HEPES 5 at pH 7.6 with NaOH. Stage V or VI oocytes were then injected with 46 nL (0.25 μg/L) of an oligonucleotide antisense to endogenous Cx38 via a Drummond nanoject apparatus (Drummond, Broomall, PA; Barrio et al., 1991). The Cx38 antisense oligonucleotide is 5′-gctttagtaattcccatcctgccatgtttc. Oocytes were maintained at 18°C for all overnight incubations. 24 to 72 hours later, the oocytes were injected with the cRNA of interest (0.2 to 1 μg/L) at the vegetal pole. Oocytes were incubated overnight at 18°C. The vitelline layer was mechanically removed after immersion in a hypertonic solution. Oocytes were paired vegetal pole to vegetal pole in a recording chamber. Electrophysiological recording proceeded 2–3 hours after pairing. All chemicals were of standard research or molecular biology grade, as appropriate.

V_j and Uncoupling Protocol

The recording chamber was continuously perfused with ND96, 0.6 mL/min, for the duration of the experimental protocol. Double voltage clamp was used for G_j measurements (Spray et al., 1981). Voltage and current electrodes were impaled into each oocyte. Both cells were clamped at $V_m = -20$ mV ($V_j = 0$ mV) by oocyte clamps (OC-725C, Warner Instruments, Hamden, CT). The current signals were split into two systems after filtering at 10 Hz and sampled at 20 Hz. One system used pCLAMP 8.2 for pulse generation and data acquisition (Digidata 1320, Axon, Union City, CA). A second system (Digidata 1200, Axon) monitored both voltage and current signals using Axoscope 8.0 (Axon). Data were graphed with SigmaPlot (SSPS, Chicago, IL) and Excel (Microsoft, Seattle, WA). All data were graphed as mean ± SEM. Appropriate Student's *t*-tests were performed, with $P < 0.05$ (two-tailed) considered as statistically significant.

At rest, both oocytes were clamped at −20 mV ($V_j = V_{m1} - V_{m2}$ or 0 mV, where V_{m1} and V_{m2} are the membrane potentials of oocytes 1 and 2, respectively), so that zero junctional current passed ($I_j = 0$). For measuring the G_j vs. V_j relationship, the following voltage protocol was used: 6 steps of increasing hyperpolarizations

(V_j steps of 20, 40, 60, 80, 100 and 120 mV), 25 s duration, were applied every 50 s to each oocyte, while the other oocyte remained clamped at −20 mV. For Cx26 channels, 10 mV incremental hyperpolarizations were used from 10 to 130 mV. V_j equals $V_{step1} - V_{m2}$. G_j is the absolute junctional current (I_j) needed to maintain the second oocyte at −20 mV, divided by V_j. Using Clampfit 8.0 (Axon), I_j current traces were fit with a single exponential decay function. The fit steady-state value (c) and time constant (τ) were used. For square pulses, the average I_j during the last 2 s of the pulse was used for G_{jss} and the average of the first second was used for G_{jpeak}. The ratio G_{jss}/G_{jmax} was plotted against V_j. All data points were graphed and fit to a two-state Boltzmann distribution: $(G_{jss} - G_{jmin})/(G_{jmax} - G_{jss}) = \exp[-A(V_j - V_o)]$, where V_o is the voltage at which half of the conductance is inactivated; G_{jmax} is G_j at $V_j = 0$ mV and G_{jmin} is the normalized theoretical minimum. $A = \eta q/kT$, where η is the number of equivalent gating charges moving through the entire applied field, q is the charge of an electron, k is the Boltzmann constant and T is the temperature in degrees Kelvin.

For all of the studies, chemical gating was achieved with perfusion of ND96 saturated with varying percentages of CO_2. For gas less than 100%, N_2 was mixed with CO_2 (Airgas East, Rochester, NY). Exposure of oocyte pairs to CO_2-saturated ND96 decreases cytoplasmic pH and increases cytoplasmic calcium concentration (Wang & Peracchia, 1997; Peracchia & Wang, 1997). To monitor V_j gating changes due to CO_2 exposure, two protocols were used. First, 12 s pulses of different V_j (range 20 to 100 mV) were applied to one oocyte every 30 s. The oocytes were exposed to ND96 bubbled continuously with 100% CO_2 for three minutes. G_j was monitored before, during and after CO_2 washout. For the second protocol, oocyte pairs were initially tested with the V_j voltage protocol (*see* above paragraph). A train of −80 mV (Cx32, Cx32-N2D) or −120 mV (Cx26) 12 s pulses was applied to one oocyte every 30 s. After a stable baseline, perfusion was switched to a second reservoir that was continuously bubbled with 30% (70% nitrogen) or 100% CO_2. After at least 15 min of CO_2 exposure, when the currents appeared to be at a new steady-state level on the Axoscope system, the voltage protocol was applied again. In some experiments, perfusion was changed back to control ND96 and G_j was monitored by applying −80 mV or −120 mV 12 s pulses every 30 s during recovery. After recovery, a third voltage protocol was applied. In all cases, G_{jpeak} and G_{jss} were normalized to G_{jpeak} at the start of the experiment; when time equaled zero s.

Results

Cx32 Wild Type

To test the effect of short CO_2 exposures on V_j closure, oocyte pairs expressing Cx32wt were superfused for three min with 100% CO_2-saturated ND96. V_j closure was monitored using 12 s, ±80 mV V_j steps applied every 30 s (Fig. 1, $n = 6$). G_{jpeak} (*triangle*) and G_{jss} (*circle*) are normalized to G_{jpeak} of the first pulse (time = 0 s) as 100%. As partial uncoupling developed, G_{jpeak} and G_{jss} decreased from 100% to 80 ± 9.2% and from 45.9% to 25.9 ± 4.2%, respectively, resulting in a drop of G_{jss}/G_{jpeak} ratio (*squares*) from ~ 0.46 ± 0.04 to 0.32 ± 0.02. The decrease in G_{jpeak} reflects the number of channels closed by CO_2, as G_{jpeak} is insensitive to V_j, whereas the drop in the ratio of G_{jss}/G_{jpeak} reflects an increase in voltage-dependent closure during the pulse. Thus, the latter

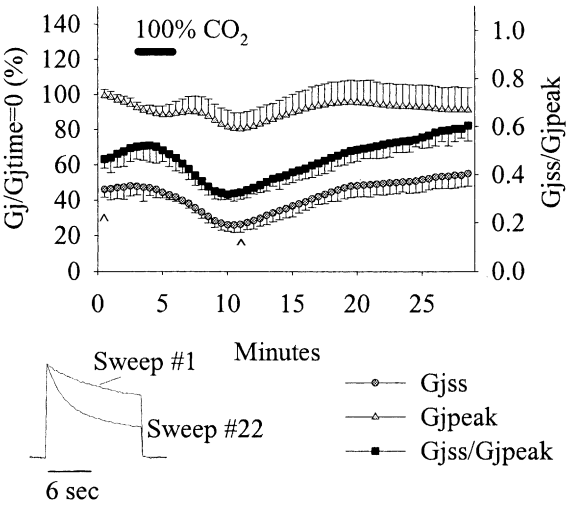

Fig. 1. Effect of CO_2 on G_j and V_j closure of Cx32 channels. Channel closure is monitored using 12 s, ± 80 mV pulses during a 3 min exposure to 100% CO_2-saturated ND96. G_{jpeak} (*triangles*) and G_{jss} (*circles*) decrease with CO_2 perfusion and recover with washout. The ratio G_{jss}/G_{jpeak} (*squares*) also decreases, indicating voltage closure during the pulse (increased V_j-dependent closure; $n = 6$). Data are mean ± SEM. *Inset*: I_j traces normalized to I_{jpeak} under control and uncoupled conditions. Data points corresponding to the traces are indicated by the ^ in the graph.

indicates that CO_2 significantly increases the closure of Cx32 channels by $V_j = 80$ mV. This is clearly seen in the inset of Fig. 1, which shows two normalized I_j traces, from a 12 s 80 mV step, before (*sweep #1*) and during (*sweep #22*) uncoupling. Traces are normalized to I_{jpeak}. Both G_{jpeak} and G_{jss}/G_{jpeak} returned to near normal values after CO_2 washout. CO_2 application also affected the kinetics of I_j inactivation, as the time constant of V_j-dependent channel closure decreased reversibly from 5.7 ± 0.9 s to 2.8 ± 0.4 s (*data not shown*).

The effects of short 100% CO_2 exposure on Cx32 channel V_j gating was also tested at additional V_j gradients. With $V_j = \pm 40$, ±60 and ±100 mV, the ratio G_{jss}/G_{jpeak} decreased during 3 min exposure to 100% CO_2-saturated ND96 (*data not shown*). In contrast, no noticeable change in V_j gating was observed with $V_j = 20$ mV; both G_{jpeak} and G_{jss} decreased slightly, such that the ratio G_{jss}/G_{jpeak} did not significantly change (*data not shown*). These data further support CO_2-mediated increases of Cx32 channel V_j gating only at V_j greater than 20 mV.

Three-minute exposure to 100% CO_2 does not create steady-state conditions (Fig. 1). Therefore, longer CO_2 exposures were used to determine in more detail the effect of CO_2 on the V_j gating of Cx32 channels (Fig. 2). The conventional V_j protocol was applied before and after reaching steady-state conditions (Fig. 3). Oocyte pairs were superfused continuously with 100% CO_2-saturated ND96 until G_j

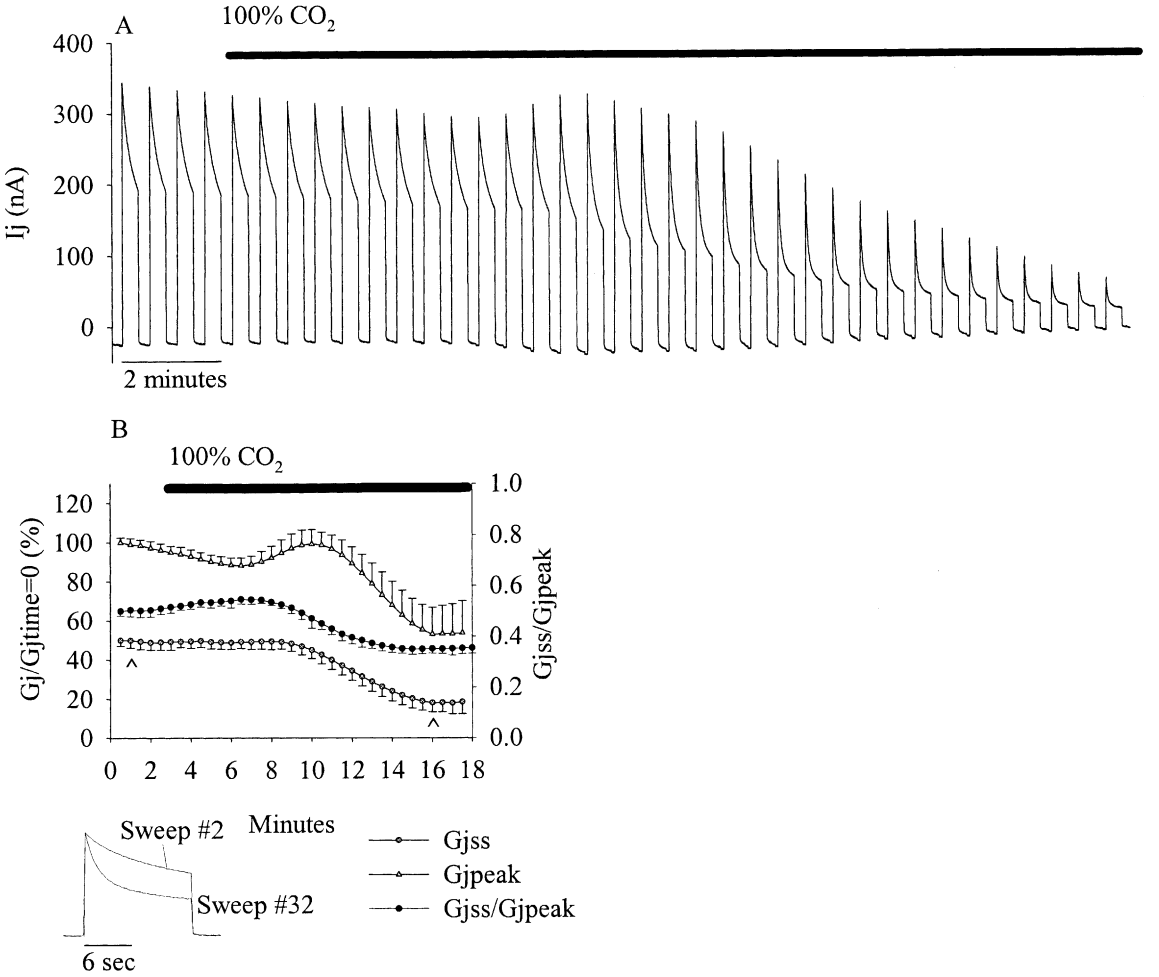

Fig. 2. G_j changes in Cx32 channels during exposure to 100% $C0_2$. (*A*) I_j from one cell pair monitored during exposure to 100% CO_2-saturated ND96 (−80 mV, 12 s pulses, every 30 s). (*B*) G_{jpeak} (*triangles*) and G_{jss} (*circles*) both decrease during chemical uncoupling but not to the same extent, such that the ratio G_{jss}/G_{jpeak} (*squares*) decreases (increased V_j closure). Data are mean ± SEM and $n = 7$. *Inset*: I_j traces normalized to I_{jpeak} under control conditions and during 100% CO_2 exposure (corresponding data points are marked by ^).

closure stabilized. Pulses of 12 s and -80 mV were applied every 30 s and both G_{jpeak} and G_{jss} were measured. Figure 2*A* shows an I_j record to illustrate the decrease in G_{jpeak} and G_{jss}, and the increased V_j closure that takes place during exposure to 100% CO_2. Steady-state conditions were reached in ~15 min. At that time, G_{jpeak} decreased from 100% to 53.2 ± 14.4% and G_{jss}, from 49.9% to 18.0 ± 4.7% (Fig. 2*B*, $n = 7$). G_{jss} and G_{jpeak} are again normalized to G_{jpeak} at time = 0 s as 100%. The ratio G_{jss}/G_{jpeak} decreased from 0.50 ± 0.02 to 0.34 ± 0.02. The inset of Fig. 2*B* illustrates the change in I_j, normalized to I_{jpeak}, with 12 s, −80 mV V_j pulses sampled before (*sweep #2*) and during (*sweep #32*) chemical uncoupling. The time course of G_{jpeak} was biphasic, increasing first before dropping, while that of G_{jss} was a monophasic drop to steady-state values (Fig. 2*A* and *B*). Because of this, G_{jss}/G_{jpeak} dropped significantly earlier than G_{jpeak} and G_{jss}. These differences in time course were also observed with 3 min exposures to CO_2 (Fig. 1*A* and *B*).

Data generated by the conventional V_j protocol, applied before and after reaching steady state in 100% CO_2, clearly demonstrate the effect of CO_2 on V_j-dependent closure. Figure 3*A* and *B* shows I_j inactivation traces at different V_j gradients (±20 mV to 120 mV in 20 mV increments, 25 s pulses) under control and chemical-gating conditions, respectively. Changes in the degree of V_j closure are illustrated in plots of the relationship between V_j and G_{jss}/G_{jmax} (Fig. 3*C*; control, *circles*, $n = 11$; CO_2, *squares*, $n = 8$; $^*P < 0.05$ vs control). Cx32 channels show significantly increased V_j closure during chemical uncoupling at ± 40, 60, 80, 100 mV and 120 mV, consistent with data obtained during the brief 3 min CO_2 exposure studies (Fig. 1). The parameters of the Boltzmann fit (Table 1) demonstrate an inward shift of V_o from ~60 mV to 41 mV, a decrease in η from

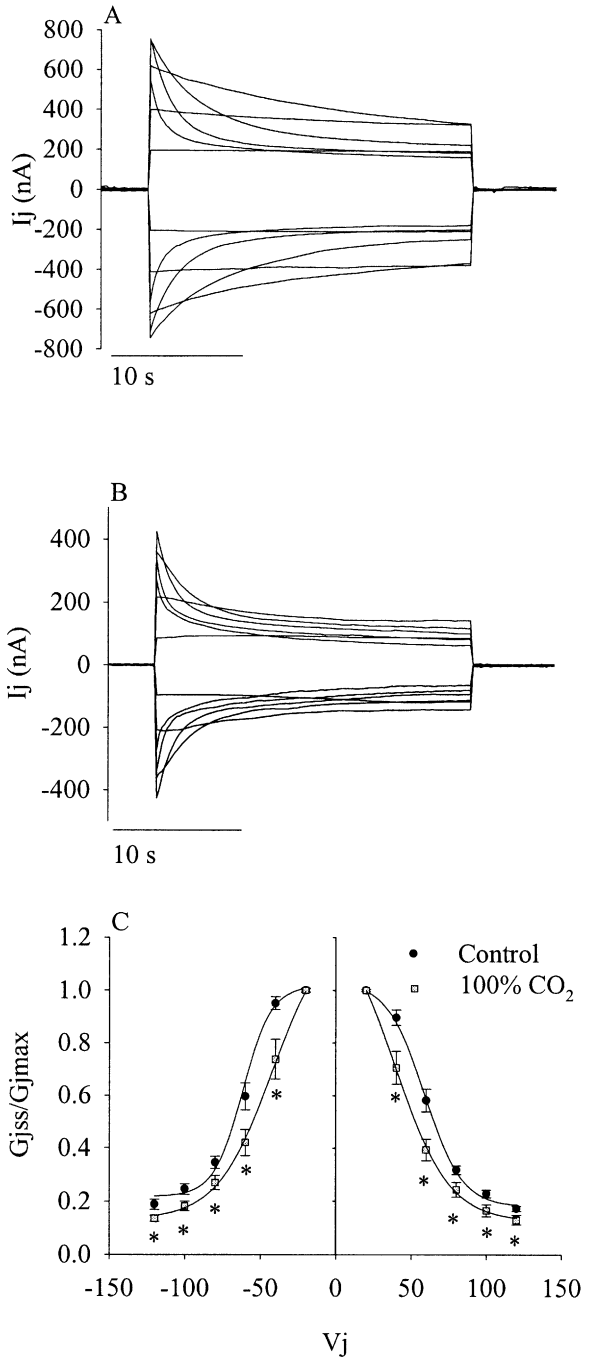

Fig. 3. V_j gating of Cx32 channels: control and during perfusion with 100% CO_2-saturated ND96. (*A*) Control I_j for Cx32 (25 s, 20 mV increments from 20 mV to 120 mV). (*B*) I_j during the voltage protocol while perfusing with 100% CO_2-saturated ND96. (*C*) G_j vs V_j for Cx32 control (*circles*, $n = 11$) and Cx32 V_j closure during exposure to 100% CO_2-bubbled ND96 (squares, $n = 8$). Data are mean ± SEM. Lines represent Boltzmann fits of the data. $^*P < 0.05$ vs control.

2.3 to 1.4, a decrease in G_{jmin} from 0.2 to 0.13 during chemical gating and an increase in G_{jmax} from 1.03 to 1.27. The 20 mV pulses under both conditions were square - no I_j inactivation - therefore the G_{jmax} for CO_2 conditions should be 1.0. In addition, I_j inactivation is much faster, as τ is significantly smaller at 40, 60, 80 and 100 mV V_j (*data not shown*). Control values of a Boltzmann fit agree with previous reports (Barrio et al., 1991; Wang et al., 1996). In contrast to a previous report (Werner et al., 1991), Cx32 channels showed no change in V_j gating during exposure to 30% CO_2-saturated ND96 (*data not shown*).

Cx26 Wild Type

Cx26 is more sensitive to CO_2 than is Cx32, since exposure to 100% CO_2-saturated ND96 closes virtually all of the channels. To evoke chemical gating without closing all of the channels, the oocytes were exposed to ND96 saturated with 30% CO_2. Pulses of 12 s, 120 mV applied every 30 s were used to monitor Cx26 channel closure and changes in V_j closure. With 30% CO_2, G_{jpeak} decreased from 100% to 47.5 ± 11.6%, whereas G_{jss} only decreased from 41.0% to 28.2 ± 6.2%, so that the ratio G_{jss}/G_{jpeak} increased from 0.41 ± 0.05 to 0.59 ± 0.02 (Fig. 4, $n = 6$). Percent conductance is the amount of conductance remaining compared to G_{jpeak} at the start of the experiment. I_j traces normalized to I_{jpeak}, sampled during control conditions (*sweep #2*) and 30% CO_2-induced chemical closure (*sweep #34*), show the decrease in V_j closure (Fig. 4, *inset*, 12 s 120 mV pulse). The time course of G_{jss}/G_{jpeak} matched reasonably well those of G_{jpeak} and G_{jss} (Fig. 4). In this, Cx26 differs from Cx32 (*see above*).

After reaching steady-state conditions in 30% CO_2, the V_j protocol was applied to determine in detail the changes in V_j-dependent closure. Figure 5*A* (*control*) and 5*B* (30% CO_2) shows I_j traces in response to 25 s, 20 mV incremental depolarizations up to 120 mV. The plot of the relationship between V_j and G_{jss}/G_{jmax} using 25 s, 10 mV incremental depolarizations from 10 mV to 130 mV demonstrates a significant decrease in V_j-dependent closure at $V_j \geq \pm 110$ mV (Fig. 5*C*; control, *circles*, $n = 8$; CO_2, *squares*, $n = 7$; $^*P < 0.05$). The parameters of the Boltzmann fit for control conditions are listed in Table 1 and agree with previously reported values (Barrio et al., 1991 ; Rubin et al., 1992). G_{jmin} increased from 0.07 to 0.16 and η decreased from 1.5 to 0.8. G_{jmax} increased from 0.98 to 1.04. V_o values did not change and there is no significant change in τ (*data not shown*). Control V_j gating returned after at least 30 min of CO_2 washout (*data not shown*). Although ±110 to ±130 mV are extreme voltages, positive-gating Cx26 channels decrease V_j-dependent closure during CO_2-induced uncoupling.

Cx32-N2D

It has been previously shown that the replacement of the neutral residue #2 (N) in the amino acid sequence

Table 1. Boltzmann parameters

	V_o	G_{jmax}	G_{jmin}	A	η	G_j
Cx32						
Control	60.2 ±1.7	1.03 ± 0.03	0.2 ± 0.03	0.091 ± 0.014	2.3	6.6 ± 1.6
100%	40.7 ± 8.8*	1.27 ± 0.25*	0.13 ± 0.04*	0.056 ± 0.017*	1.4	
Cx26						
Control	98.7 ± 3.4	0.98 ± 0.02	0.07 ± 0.06	0.061 ± 0.009	1.5	5.8 ± 1.3
30%	98.0 ± 3.4	1.04 ± 0.01*	0.16 ± 0.05*	0.033 ± 0.003*	0.8	
Cx32N2D						
Control	63.8 ± 2.3	0.99 ± 0.03	0.21 ± 0.03	0.099 ± 0.022	2.5	7.0 ± 1.3
30%	72.7 ± 3.3*	1.01 ± 0.04	0.33 ± 0.05*	0.065 ± 0.015*	1.6	

*$P < 0.05$.

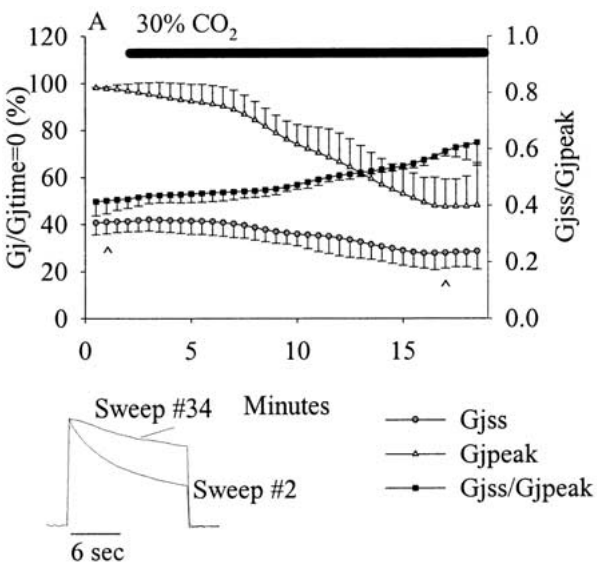

Fig. 4. G_j changes in Cx26 channels during exposure to 30% CO_2. G_{jpeak} (*triangles*) and G_{jss} (*circles*) both decrease with CO_2, but not to the same extent, such that the ratio G_{jss}/G_{jpeak} (*squares*) increases. 12 s, 120 mV V_j pulses applied every 30 s are used to measure the changes in V_j during chemical uncoupling ($n = 6$). Data are mean ± SEM. *Inset*: I_j traces normalized to I_{jpeak} from control and chemically uncoupled conditions; corresponding data points are marked by ^.

of Cx32 with a negatively charged one (D) switches the polarity of the fast V_j sensor from negative to positive (Verselis et al., 1994; Oh et al., 1999). Experiments testing the V_j profile of heterotypic Cx32/Cx32-N2D pairs (*data not shown*) confirmed that the mutant Cx32-N2D becomes a positive gater and were similar to a previous report (Oh et al., 1999).

As predicted by the hypothesis, the V_j closure to pulses of 12 s, 80 mV Cx32-N2D homotypic channels decreased significantly with CO_2 application. G_{jpeak} decreased from 100% to 20.2 ± 1.6% and G_{jss} decreased from 59.6% to 18.4 ± 20.0% during chemical uncoupling with 100% CO_2-saturated ND96. This caused G_{jss}/G_{jpeak} to increase from 0.60 ± 0.02 to 0.91 ± 0.01 (Fig. 6; $n = 3$). G_{jss} and G_{jpeak} are normalized to G_{jpeak} at the start of the experiment as 100%. The two current traces (12 s, −80 mV pulses), normalized to I_{jpeak}, clearly display the reduced I_j inactivation in the presence of 100% CO_2 (Fig. 6, *inset*). Of note, the time course of G_{jss}/G_{jpeak} matched reasonably well those of G_{jpeak} and G_{jss} (Fig. 6). In this, Cx32-N2D behaves similarly to Cx26, but differs from Cx32 (*see* above).

To study in more detail the effect of CO_2 on V_j closure, the V_j protocol was applied before and after reaching steady-state conditions in 30% or 100% CO_2. I_j traces elicited by application of 25 s, 20 to 120 mV V_j pulses for control (Fig. 7*A*), 30% (Fig. 7*B*) and 100% (Fig. 7*C*) CO_2-saturated ND96 show a progressive decrease in I_j inactivation. Plots of the relationship between V_j and G_{jss}/G_{jmax} demonstrate decreased V_j closure at ±80, 100 and 120 mV V_j for both 30% (*triangles*, $n = 8$) and 100% CO_2 (*squares*, $n = 7$)-saturated ND96 compared to control (Fig. 7*D*; *circles*, $n = 13$; *$P < 0.05$). The values of the Boltzmann fits (Table 1) show that V_o increases from ~64 to 73 mV, η decreases from 2.5 to 1.6 and G_{jmin} increases from 0.21 to 0.33 with exposure to 30% CO_2-saturated ND96. Data from experiments with 100% CO_2 were not well fit by the Boltzmann equation because no minimum was reached with ±120 mV V_j pulses.

Values for τ for Cx32-N2D were inconsistent. Tau increased or decreased versus control with different V_j steps and CO_2 concentrations. More work is needed to determine the effect of chemical gating on τ for Cx32-N2D. The point mutation Cx32-N2D generates a positive-gating Cx32 mutant. This mutant decreases V_j closure during chemical uncoupling, providing direct evidence for our hypothesis.

V_j gating recovered to control values after prolonged washout of 30% CO_2 (*data not shown*). Recovery data could not be obtained after exposure to 100% CO_2 because G_j increased beyond 40 μS during washout for longer than 20 min ($n = 3$, *data not shown*).

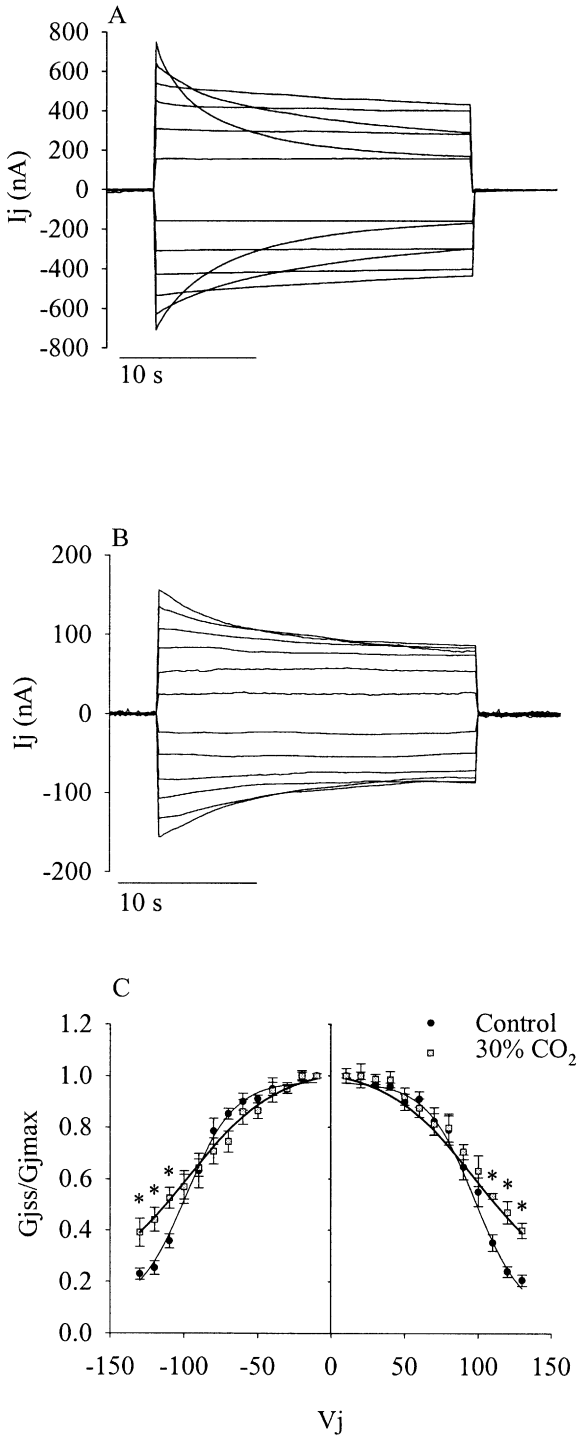

Fig. 5. V_j gating of Cx26 channels: control and during perfusion with 30% CO_2-saturated ND96. (*A*) I_j traces from the V_j protocol (25 s, 20 mV to 120 mV in 20 mV steps shown only) under control conditions. (*B*) I_j traces from the V_j protocol, 10 mV steps from 10 mV to 130 mV, during exposure to 30% CO_2-saturated ND96. (*C*) G_j vs V_j for Cx26 control (*circles*, $n = 8$) and 30% CO_2 (*triangles*, $n = 7$). Data are mean ± SEM. Lines represent Boltzmann fits of the data, $*P < 0.05$ vs control.

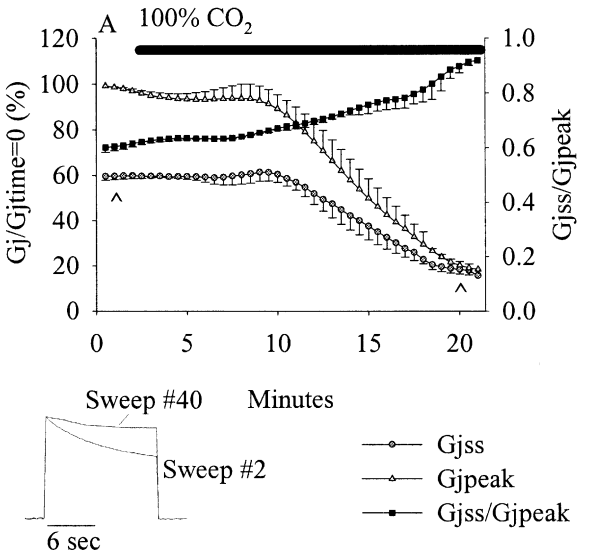

Fig. 6. G_j changes in Cx32N2D channels during exposure to 100% CO_2. Both G_{jpeak} (*triangles*) and G_{jss} (*circles*) decrease during exposure to 100% CO_2-saturated ND96, but by different amounts, such that the ratio (G_{jss}/G_{jpeak}, *squares*) increases (reduced V_j-dependent closure). 12 s, 80 mV V_j pulses applied every 30 s are used to measure the changes in V_j during chemical uncoupling ($n = 3$). Data are mean ± SEM. *Inset*: I_j traces normalized to I_{jpeak} under control and chemically uncoupled conditions; corresponding data points are denoted by ^.

Cx26-D2N

In Cx26, the point mutation, Cx26-D2N, switches the gating polarity of Cx26 channels from positive to negative (Verselis et al., 1994; Oh et al., 1999). Functional Cx26-D2N channels, tested heterotypically against Cx26 wild type, displayed V_j gating similar to that previously reported (Oh et al., 1999), confirming the switch in V_j gating polarity (*data not shown*). Unfortunately, homotypic Cx26-D2N/Cx26-D2N pairs did not result in measurable G_j. This is consistent with a previous report, in which it was suggested that the channels may reside in a low-conductance substate (Oh et al., 1999). Homotypic pairing of two channels, both in substates, would greatly reduce G_j, decreasing dramatically the signal-to-noise ratio.

Discussion

This study shows that CO_2-induced chemical gating affects, in opposite ways, the V_j closure of Cx32 and Cx26 channels. CO_2 increases V_j closure of Cx32 and decreases that of Cx26 channels. A summary of selected results is shown in Fig. 8. For 80 mV and 120 mV pulses, G_{jss}/G_{jmax} of negative-gating Cx32 channels decreased significantly from 0.33 ± 0.02 to 0.26 ± 0.03 and from 0.18 ± 0.01 to 0.13 ± 0.01, respectively, during uncoupling with CO_2 ($*P <$

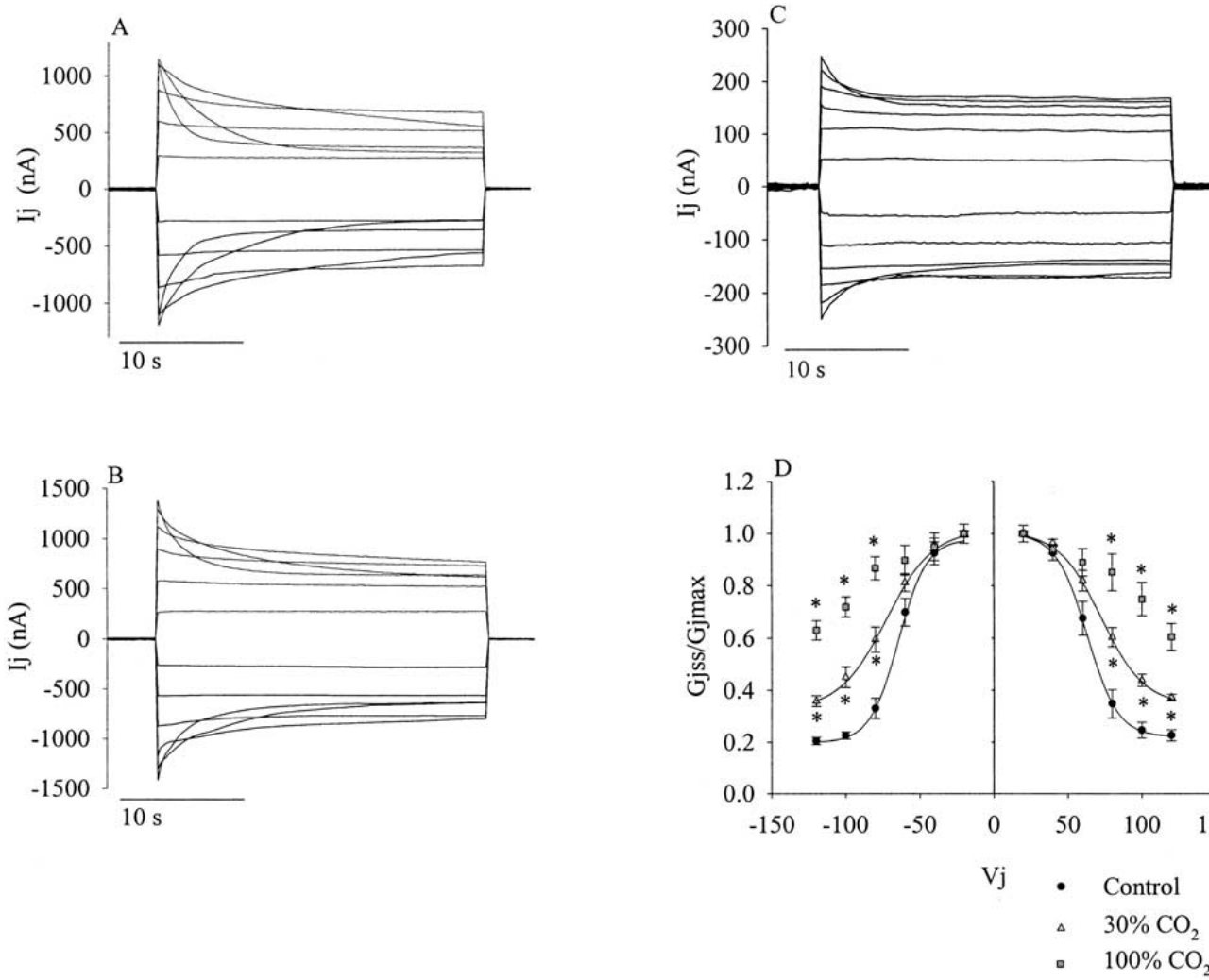

Fig. 7. V_j gating of Cx32N2D channels: control and during perfusion with 30% or 100% CO_2-saturated ND96. I_j traces from the V_j protocol —25 s, 20 mV increment depolarizations from 20 to 120 mV — for control (*A*), 30% CO_2 (*B*) and 100% CO_2 (*C*). (*D*) G_j vs V_j graphs for control (*circles*, $n = 13$), 30% CO_2 (*triangles*, $n = 8$) and 100% CO_2 (*squares*, $n = 7$). Data are mean ± SEM. Lines represent Boltzmann fits. $^*P < 0.05$ vs control.

0.05 versus control). G_{jss}/G_{jmax} increased for positive-gating Cx26 from 0.25 ± 0.02 to 0.46 ± 0.05 (Fig. 8, only 120 mV shown; $^*P < 0.05$ versus control). In addition, a Cx32 point mutation (Cx32-N2D) that inverts gating polarity also inverts the V_j gating response to CO_2. G_{jss}/G_{jmax} for Cx32-N2D channels is significantly increased with perfusion of both 30% and 100% CO_2 (Fig. 8, only 80 mV and 120 mV are shown). For 80 mV pulses, G_{jss}/G_{jmax} increased from 0.34 ± 0.05 to 0.60 ± 0.04 and from 0.86 ± 0.06 with 30% and 100% CO_2, respectively. G_{jss}/G_{jmax} increased from 0.22 ± 0.02 to 0.37 ± 0.02 and from 0.62 ± 0.04 with 100 mV pulses. The opposite effect of CO_2 appears to be related to the polarity of V_j gating, as Cx32 channels gate at the negative side of V_j, while Cx26 and Cx32-N2D channels gate at the positive side of V_j.

V_j gating changes during CO_2 perfusion are not solely a phenomenon that occurs during steady-state chemical uncoupling. Short, 3 min, exposure to CO_2 also changed the G_{jss}/G_{jpeak} ratio of 80 mV pulses (Fig. 1). Changes in G_{jss}/G_{jpeak} during brief exposures are comparable to the steady-state data because G_{jss}/G_{jpeak} changes with $V_j = 40$, 60, 80 and 100 mV pulses, but not with 20 mV pulses.

Interestingly, the onset of increased Cx32 channel V_j closure precedes that of CO_2-induced channel closure (chemical gating). This is demonstrated by the drop in G_{jpeak} beginning several minutes after the drop in both G_{jss} and G_{jss}/G_{jpeak}. Since G_{jpeak} reflects the activation of the chemical gate, this asynchrony may indicate that different mechanisms play a role in the effect of CO_2 on V_j- and chemical gating of Cx32 channels. Also, a similar asynchrony between chem-

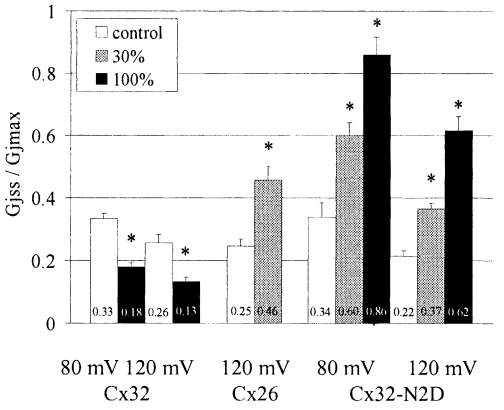

Fig. 8. Summary: G_{jss}/G_{jmax} from the V_j protocol for Cx32, 80 mV and 120 mV pulses; Cx26, 120 mV pulses; and Cx32-N2D, 80 mV and 120 mV pulses under control (*white*), 30% CO_2 (*gray*) or 100% CO_2 (*black*) uncoupled conditions. $^*P < 0.05$ versus control.

ical gating and V_j gating to CO_2 was observed in Cx45 channels (Peracchia et al., 2003b), which are also negative gaters. The biphasic time course of G_{jpeak}—initial increase followed by a drop — suggests that CO_2 may initially increase open-channel probability and/or single-channel conductance before activating chemical gating. This biphasic time course was not observed for positive-gating Cx26 or Cx32-N2D channels. The mechanism behind this phenomenon is still unclear, but it cannot be studied in oocytes because single-channel events cannot be monitored in this assay system.

CO_2 has the opposite effect on Cx26 channels, as their V_j closure decreases during partial chemical uncoupling induced by 30% CO_2. This decrease, however, is only observed at high voltages ($V_j > \pm 100$ mV). Although these are extreme voltages, the effect of CO_2 is present and statistically significant. Higher CO_2 concentrations are perhaps needed for the effect of CO_2 to manifest itself at lower V_j values. However, CO_2 concentrations higher than 30% could not be tested because they closed all of the channels, such that steady-state conditions with sufficient numbers of operational channels could not be attained.

The difference in the effects of CO_2 on V_j gating among connexin channels is likely to be related to the polarity of fast V_j gating. Indeed, CO_2 increases V_j-dependent closure of negative gaters, such as Cx32 (this study) and Cx45 (Peracchia et al., 2003b), and decreases that of positive gaters, such as Cx26 (this study and Peracchia et al., 2003a), Cx37 (Peracchia, *unpublished data*), Cx40 (Peracchia et al., 2004), and Cx50 (Peracchia, *unpublished data*). This hypothesis is supported by evidence that a Cx32 mutation (Cx32-N2D), which inverts the gating polarity, also inverts the CO_2 effects on V_j gating. Significantly, the N2D point mutation does not affect V_j gating properties under control conditions (absence of CO_2), as the Boltzmann parameters for Cx32 and Cx32-N2D are almost identical (Table 1). The addition of a negative charge in position 2 changes the polarity and the way fast V_j gating responds to CO_2, without affecting the function of the fast V_j gate itself.

In contrast, the Cx32-N2D mutation has some effect on chemical gating. These channels are more sensitive to CO_2 than are Cx32 wild-type channels, as G_{jpeak} drops to ~20% of control values in Cx32-N2D channels and only to ~50% in Cx32 channels. Previous chemical gating studies focused on the CL (cytoplasmic loop) and CT regions of Cx32 (reviewed in Peracchia, Wang & Peracchia, 2000a). Other NT point mutations and chimeric proteins with Cx45 reveal a novel role for this region in CO_2-mediated chemical gating of Cx32 channels (Young & Peracchia, 2002; Young and Peracchia, personal communication). The role of the NT in chemical gating requires further study.

Changes in the Boltzmann parameters G_{jmin} and V_o are used to characterize the V_j response of gap junction channels. Consistent with the hypothesis, the Boltzmann fit of the means shows a decreased G_{jmin} for the negative-gating Cx32 channels from 0.2 to 0.13. Also consistent with increased V_j closure is the inward shift of V_o by ~19 mV. For positive Cx32-N2D channels, G_{jmin} increases from 0.21 to 0.33. The V_o for Cx32-N2D channels shows an outward shift of ~9 mV with 30% CO_2. The data from 100% CO_2 did not reach a minimum over the voltage range tested and thus could not be fit by the Boltzmann equation. For Cx32 and Cx32-N2D channels, the shifts in V_o and changes to G_{jmin} support more and less V_j-dependent closure during chemical uncoupling, respectively. For Cx26, the decreased closure at $V_j \geq 110$ mV with 30% CO_2 indicates less V_j closure for these positive-gating connexin channels.

Although gating polarity plays a role in determining how V_j gating is altered by CO_2 application, the mechanism involved is still unclear. This study on the effect of CO_2 on V_j gating opens new avenues for understanding gating mechanisms. Models and further studies should consider potential interplay between chemical and voltage gates.

One possible model is that protonation of a residue relevant to the function of the fast V_j gate sensor stabilizes or destabilizes the sensor, depending on the connexin's gating polarity. The mechanism of the fast V_j sensor triggering fast V_j gating is not yet fully understood. However, movement of a sensor domain comprising the first 10 amino acids of the NH_2-terminus is believed to be within the electrical field and is a likely candidate (Purnick et al., 2000). Since the internal pH of oocytes does not drop below ~6.4, even with prolonged exposure to 100% CO_2 (Wang & Peracchia, 1997), it is likely that cytosolic acidification results in histidine (H) protonation. Potential candidates for histidine protonation include the fairly

well-conserved amino acids #16, 73, 94 and 97 of Cx32 and #16, 72 and 93 of Cx26.

In conclusion, this study shows that the V_j closure of Cx32 and Cx26 channels is altered in opposite ways by exposure to CO_2. With CO_2 the voltage closure of Cx32 increases, whereas that of Cx26 decreases. It is likely that the opposite effect of CO_2 on these connexins is related to the polarity of fast V_j gating, as Cx32 and Cx26 are sensitive to negative and positive potentials, respectively. This hypothesis is supported by evidence that a Cx32 mutation (Cx32-N2D) that inverts gating polarity also inverts the response of V_j to CO_2, resulting in decreased V_j-dependent closure. The mechanism behind the effect of CO_2 on V_j gating is still unclear, but protonation of histidine residues may play a role. This study also highlights the need for caution in studying V_j and chemical gating, as these two functions may be less independent than generally thought.

We thank J.T. Chen and L.M. Peracchia for excellent technical assistance. This work is supported by NIH, grant R01-GM20113 to C. Peracchia, and in part by a NYS AHA Predoctoral Fellowship 0010078T to K. Young.

References

Barrio, L.C., Suchyna, T., Bargiello, T., Xu, L.X., Roginski, R.S., Bennett, M.V.L., Nicholson, B.J. 1991. Gap junctions formed by connexins 26 and 32 alone and in combination are differently affected by applied voltage. *Proc. Natl. Acad. Sci. USA* **88:**8410–8414

Bukauskas, F.F., Peracchia, C. 1997. Two distinct gating mechanisms in gap junction channels: CO_2-sensitive and voltage-sensitive. *Biophys. J.* **72:**2137–2142

Bukauskas, F.F., Verselis, V. 2004. Gap junction channel gating. *Biochim. Biophys. Acta.* **1662:**42–60

Bukauskas, F.F., Vogel, R., Weingart, R. 1997. Biophysical properties of heterotypic gap junctions newly formed between two types of insect cells. *J. Physiol.* **499:**701–713

Delmar, M., Stergiopoulos, K., Homma, N., Calero, G., Morley, G., Ek-Vitorin, J.F., Taffet, S.M. 2000. A molecular model for the chemical regulation of connexin43 channels: the "ball-and-chain" hypothesis. *In:* Peracchia, C, editor Gap Junctions. Molecular Basis of Cell Communication in Health, Disease. pp 223–248, Academic Press, San Diego, CA

Gilula, N.B., Reeves, O.R., Steinbach, A. 1972. Metabolic coupling, ionic coupling and cell contacts. *Nature* **235:**262–265

Harris, A.L. 2001. Emerging issues of connexin channels: Biophysics fills the gap. *Quart. Rev. Biophys.* **34:**325–472

Loewenstein, W.R. 1966. Permeability of membrane junctions. *Ann. N. Y. Acad. Sci.* **137:**441–472

Oh, S., Rubin, J.B., Bennett, M.V.L., Verselis, V.K., Bargiello, T.A. 1999. Molecular determinants of electrical rectification of single channel conductance in gap junctions formed by connexins 26 and 32. *J. Gen. Physiol.* **114:**339–364

Peracchia, C. 2004. Chemical gating of gap junction channels; roles of calcium, pH and calmodulin. *Biochim. Biophys. Acta* **1662:**61–80

Peracchia, C., Chen, J.T., Peracchia, L.L. 2004. CO_2 sensitivity of voltage gating and gating polarity of gap junction channels — Connexin40 and its COOH-terminus truncated mutant. *J. Membr. Biol.* **200:**105–113

Peracchia, C., Wang, X.G. 1997. Connexin domains relevant to the chemical gating of gap junction channels. *Braz. J. Med. Biol. Res.* **30:**577–590

Peracchia, C., Wang, X.G., Peracchia, L.L. 1999. Is the chemical gate of connexins voltage sensitive? Behavior of Cx32 wild-type and mutant channels. *Am. J. Physiol.* **276:**C1361–C1373

Peracchia, C., Wang, X.G., Peracchia, L.L. 2000a. Behavior of chemical- and slow voltage-sensitive gating of connexin channels: the "cork" gating hypothesis. *In:* Peracchia, C, editor Gap Junctions. Molecular basis of cell communication in health and disease. pp 271–295, Academic Press, San Diego, CA

Peracchia, C., Wang, X.G., Peracchia, L.L. 2000b. Chemical gating of gap junction channels. *Methods* **20:**188–195

Peracchia, C., Young, K.C., Wang, X.G., Chen, J.T., Peracchia, L.L. 2003a. The voltage gates of connexin channels are sensitive to CO_2. *Cell Commun. Adhes.* **10:**233–237

Peracchia, C., Young, K.C., Wang, X.G., Peracchia, L.L. 2003b. Is the voltage gate of connexins CO_2-sensitive? Cx45 channels and inhibition of calmodulin expression. *J. Membrane Biol.* **195:**53–62

Purnick, P.E.M., Oh, S.H., Abrams, C.K., Verselis, V.K., Bargiello, T.A. 2000. Reversal of the gating polarity of gap junctions by negative charge substitutions in the N-terminus of connexin 32. *Biophys. J.* **79:**2403–2415

Rubin, J.B., Verselis, V.K., Bennett, M.V.L., Bargiello, T.A. 1992. A domain substitution procedure and its use to analyze voltage dependence of homotypic gap junctions formed by connexins 26 and 32. *Proc. Natl. Acad. Sci. USA* **89:**3820–3824

Rose, B., Loewenstein, W.R. 1975. Permeability of cell junction depends on local cytoplasmic calcium activity. *Nature.* **254:**250–252

Sambrook, J., Fritsch, E.F., Maniatis, T. 1989. Molecular Cloning: A Laboratory Manual. Cold Spring Harbor Laboratory Press, Woodbury

Spray, D.C., Harris, A.L., Bennett, M.V.L. 1981. Equilibrium properties of a voltage-dependent junctional conductance. *J. Gen. Physiol.* **77:**77–93

Turin, L., Warner, A.E. 1977. Carbon dioxide reversibly abolishes ionic communication between cells of early amphibian embryo. *Nature* **270:**56–57

Verselis, V.K., Ginter, C.S., Bargiello, T.A. 1994. Opposite voltage gating polarities of two closely related connexins. *Nature* **368:**348–351

Wang, X.G., Li, L.Q., Peracchia, L.L., Peracchia, C. 1996. Chimeric evidence for a role of the connexin cytoplasmic loop in gap junction channel gating. *Pfluegers Arch.* **431:**844–852

Wang, X.G., Peracchia, C. 1997. Positive charges of the initial C-terminus domain of Cx32 inhibit gap junction gating sensitivity to CO_2. *Biophys. J.* **73:**798–806

Werner, R., Levine, E., Rabadan-Diehl, E., Dahl, G. 1991. Gating properties of connexin32 cell-cell channels and their mutants expressed in *Xenopus* oocytes. *Proc. R. Soc. Lond. [Biol.]* **243:**5–11

Young, K.C., Peracchia, C. 2002. Carbon dioxide sensitive voltage gating of connexin 32 and connexin32/45 chimeric channels. *Mol. Biol. Cell* **13:**351a